International Journal of Nanomedicine

Dovepress
open access to scientific and medical research

Open Access Full Text Article

ORIGINAL RESEARCH

The effect of magnetic nanoparticles on neuronal differentiation of induced pluripotent stem cell-derived neural precursors

This article was published in the following Dove Press journal:
International Journal of Nanomedicine
24 November 2016
Number of times this article has been viewed

Klára Jiráková[1]
Monika Šeneklová[1,2]
Daniel Jirák[3,4]
Karolína Turnovcová[1]
Magda Vosmanská[5]
Michal Babič[6]
Daniel Horák[6]
Pavel Veverka[7]
Pavla Jendelová[1,2]

[1]Department of Neuroscience, Institute of Experimental Medicine, Academy of Sciences of the Czech Republic, [2]Department of Neuroscience, Second Faculty of Medicine, Charles University, [3]MR-Unit, Radiodiagnostic and Interventional Radiology Department, Institute for Clinical and Experimental Medicine, [4]Department of Biophysics, Institute of Biophysics and Informatics, First Faculty of Medicine, Charles University, [5]Department of Analytical Chemistry, University of Chemistry and Technology, [6]Department of Polymer Particles, Institute of Macromolecular Chemistry, [7]Department of Magnetics and Superconductors, Institute of Physics, ASCR, Prague, Czech Republic

Introduction: Magnetic resonance (MR) imaging is suitable for noninvasive long-term tracking. We labeled human induced pluripotent stem cell-derived neural precursors (iPSC-NPs) with two types of iron-based nanoparticles, silica-coated cobalt zinc ferrite nanoparticles (CZF) and poly-L-lysine-coated iron oxide superparamagnetic nanoparticles (PLL-coated γ-Fe_2O_3) and studied their effect on proliferation and neuronal differentiation.

Materials and methods: We investigated the effect of these two contrast agents on neural precursor cell proliferation and differentiation capability. We further defined the intracellular localization and labeling efficiency and analyzed labeled cells by MR.

Results: Cell proliferation was not affected by PLL-coated γ-Fe_2O_3 but was slowed down in cells labeled with CZF. Labeling efficiency, iron content and relaxation rates measured by MR were lower in cells labeled with CZF when compared to PLL-coated γ-Fe_2O_3. Cytoplasmic localization of both types of nanoparticles was confirmed by transmission electron microscopy. Flow cytometry and immunocytochemical analysis of specific markers expressed during neuronal differentiation did not show any significant differences between unlabeled cells or cells labeled with both magnetic nanoparticles.

Conclusion: Our results show that cells labeled with PLL-coated γ-Fe_2O_3 are suitable for MR detection, did not affect the differentiation potential of iPSC-NPs and are suitable for in vivo cell therapies in experimental models of central nervous system disorders.

Keywords: neural precursors, magnetic resonance imaging, cell differentiation, superparamagnetic iron oxide nanoparticles, ferrites

Introduction

Stem cell-based therapy is a promising approach for the treatment of various central nervous system (CNS) disorders.[1] Parkinson's disease (PD) is the most common neurodegenerative movement disorder characterized pathologically by degeneration of the dopaminergic (DA) neurons in the substantia nigra.[2,3] Mouse and human induced pluripotent stem cells (iPSCs) and embryonic stem cells (ESCs) can be in vitro differentiated into various cell types relevant for regenerative medicine, eg, to specific subtypes of neurons such as motor or DA.[4,5] DA neurons were also applied in in vivo applications in rat or mouse disease models.[6,7] Cell replacement therapy in PD might restore DA neurotransmission when transplanted to the DA-depleted striatum.[8] Human iPSC-derived neural precursors (iPSC-NPs)[9] offer a source for cell transplantation therapy in CNS disorders, while minimizing the risk of tumorigenesis present with pluripotent ESCs and iPSCs.[10,11] For in vivo application and translation into the clinic, alongside standard histological and immunohistochemical methods, there is a need for

Correspondence: Pavla Jendelová
Department of Neuroscience, Institute of Experimental Medicine, ASCR, Vídeňská 1083, 142 20 Prague 4, Czech Republic
Tel +420 241 062 828
Fax +420 241 062 706
Email jendel@biomed.cas.cz

submit your manuscript | www.dovepress.com
Dovepress
http://dx.doi.org/10.2147/IJN.S116171

long-term monitoring of transplanted cells. For theranostic success and for determining the safety of cell-based therapy, it is crucial to assess the engraftment, distribution pattern, differentiation and cell survival of injected cells. Magnetic resonance (MR) imaging can confirm the technical success of transplantation and makes possible noninvasive long-term and repeated tracking. MR imaging has been well established as a useful approach for tracking neural progenitor cells transplanted in animal models for therapeutic purposes.[12,13] In order to visualize the transplanted stem cells, the cells need to be labeled with a contrast agent that enhances the contrast before transplantation. Cell labeling involves the uptake of magnetic particles into the cell cytoplasma.[14,15] Despite the beneficial role of a contrast agent for monitoring grafted cells, it is crucial to analyze the effects of magnetic nanoparticles on cell viability, function and differentiation prior to in vivo experiments.[16] In this study, we investigated the effect of two different contrast agents on neural precursor cell proliferation and differentiation capability. We also defined intracellular localization and labeling efficiency and visualized labeled cells using MR. We used two types of magnetic nanoparticles: 1) silica-coated cobalt zinc ferrite nanoparticles ($Co_{0.5}Zn_{0.5}Fe_2O_{4+\gamma}$) (CZF),[17] and 2) superparamagnetic iron oxide nanoparticles (SPIONs) – maghemite (γ-Fe_2O_3) coated with poly-L-lysine (PLL-coated γ-Fe_2O_3).[18] These particles mainly reduce T_2 and T_2* relaxation time on the MR imaging, so they could be detected as a hypointense signal on T_2 and T_2*-weighted MR images.

Materials and methods

Human iPSC-NPs and differentiation into DA neurons

The human iPSC line was derived from female (IMR90) human fetal lung fibroblasts (ATCC, Manassas, VA, USA) transduced according to Yu et al[19] with a lentivirus-mediated combination of OCT4, SOX2, NANOG and LIN28 human complementary DNA (cDNA). Clone selection, validation of the iPSC line and derivation of neuronal precursors are described in detail by Polentes et al.[20] Briefly, early neural precursors were produced in low-attachment culture in the presence of Noggin (500 ng/mL) (R&D Systems, Minneapolis, MN, USA), the transforming growth factor-β pathway inhibitor SB 431542 (10 nM) (Sigma-Aldrich Co., St Louis, MO, USA), basic fibroblast growth factor (bFGF; 10 μg/mL) and brain-derived neurotrophic factor (BDNF; 20 μg/mL) (both from PeproTech, London, UK). The human iPSC-NPs were routinely cultured in tissue culture flasks coated with poly-L-ornithine (0.002% in distilled water) and laminin (10 μg/mL in Dulbecco's Modified Eagle's Medium [DMEM]:F12), both from Sigma-Aldrich Co. Growth media comprising DMEM:F12 and neurobasal medium (1:1), B27 supplement (1:50), N2 supplement (1:100) (Gibco, Life Technologies, Grand Island, NY, USA), primocin (100 μg/mL) (InvivoGen, San Diego, CA, USA), FGF (10 ng/mL), epidermal growth factor (10 ng/mL) and BDNF (20 ng/mL) (PeproTech) were changed three times per week. Differentiation into DA neurons was performed according to the protocol by Cho et al.[21] Briefly, neural precursors were cultured in differentiating media containing DMEM:F12, B27 supplement (1:50), N2 supplement (1:100), nonessential amino acids (1%) (Gibco, Life Technologies), L-glutamine 1 mM (Sigma-Aldrich Co.), 2-mercaptoethanol 0.1 mM and primocin (100 μg/mL). The fourth day after culturing in differentiating media, SHH (200 ng/mL) and FGF8 (100 ng/mL) (PeproTech) were added. The medium was changed every second day. On the eighth day, ascorbic acid (200 μM) and retinoic acid (5×10^{-5} M) (Sigma-Aldrich Co.) were added, and the medium was changed every second day for 14 days.

Iron oxide nanoparticles and cell labeling

Two types of nanoparticles were used for cell labeling of iPSC-NPs, CZF and PLL-coated γ-Fe_2O_3. CZF were prepared by the Laboratory of Oxide Material, Department of Magnetics and Superconductors, Institute of Physics, ASCR, v. v. i.; the core is made up of Co, Zn and Fe, and it is coated with silicone dioxide. PLL-coated γ-Fe_2O_3 were prepared by the Laboratory of Polymer Particles, Centre of Biomolecular and Bioanalogous Systems, Institute of Macromolecular Chemistry of the Czech Academy of Sciences, and composed of γ-Fe_2O_3, coated with poly-L-lysine. Detailed nanoparticle preparation is described by Novotna et al[22] and Babič et al[18]. Both types of nanoparticles were used in concentrations (5, 10 and 15 μg Fe/mL in cultivation media), and the cells were incubated with a contrast agent for 72 hours. After this period, the medium was removed, and the cells were washed three times with phosphate-buffered saline (PBS) and used in further experiments. Prior to differentiation, we labeled cells with 15 μg Fe/mL in cultivation media for both types of nanoparticles for 72 hours. As a control, we refer to unlabeled cells.

Cell proliferation analysis

To investigate the effect of CZF and PLL-coated γ-Fe_2O_3 on iPSC-NP proliferation, a real-time measurement proliferation assay was used. Cells were monitored using the xCELLigence RTCA Instrument (ACEA Biosciences, San Diego, CA,

USA). In the system, the electrode impedance, which is displayed as cell index values, is used to monitor cell viability, growth and morphology and adhesion degree. In the experiment, 20,000 iPSC-NPs were seeded in the E plate wells coated with poly-L-ornithine and laminin. The cell proliferation in the presence of different concentrations (5, 10 and 15 μg Fe/mL in cultivation media) of both types of nanoparticles was measured over a time period of 72 hours; the impedance was recorded in 15-min intervals. All experiments were done in duplicates and repeated three times. Statistical analyses were performed with Student's *t*-test.

Labeling efficiency

To assess the labeling efficiency, iPSC-NP cells were incubated with different concentrations (5, 10 and 15 μg Fe/mL in cultivation media) of CZF or PLL-coated γ-Fe_2O_3 for 72 hours. The cells were then washed three times with PBS to remove floating nanoparticles. The cells were trypsinized and collected for cytospin slide preparation. For Prussian blue (PB) staining, cells were fixed in ice-cold methanol for 5 min, incubated for 30 min with 2% potassium ferrocyanide in 6% hydrochloric acid, washed and counterstained with nuclear fast red. Slides were examined using a ZEISS AXIO Observer D1 microscope (Carl Zeiss, Weimar, Germany) and analyzed with the Image J program (National Institutes of Health, Bethesda, MD, USA).

At least 300 cells were counted per sample. The experiment was repeated three times. Statistical analyses were performed with *t*-test.

Electron microscopy

Nanoparticle localization inside the non-differentiating and differentiating cells was verified by transmission electron microscopy (TEM). Non-differentiating cells were incubated with nanoparticles for 72 hours (at a concentration of 15 μg Fe/mL culture media) and then subjected to electron microscopy. Differentiating cells were incubated with nanoparticles for 72 hours and then differentiated according to the protocol described earlier. Cells were then fixed with 2.5% glutaraldehyde in 0.1 M Sörensens buffer for 72 hours at 4°C and stained using 1% osmium tetraoxide in 0.1 M Sörensens buffer for 2 hours. Then, they were dehydrated in ethanol, immersed in propylene oxide and flat embedded in Epon 812 using gelatin capsules. After polymerization for 72 hours at 60°C, the coverslips were removed using liquid nitrogen. Ultrathin sections of 60 nm were examined with a Philips Morgagni 268D transmission electron microscope (FEI Inc., Hillsboro, OR, USA).

Inductively coupled plasma mass spectrometry (ICP-MS)

The iPSC-NPs were incubated for 72 hours with CZF and PLL-coated γ-Fe_2O_3 in concentrations of 5, 10 and 15 μg Fe/mL. Before harvesting, the cells were washed three times with PBS to remove floating nanoparticles. The cells were counted in hemocytometer and then resuspended in distilled water. The samples were quantitatively transferred by concentrated nitric acid into Teflon containers for microwave digestion. A mixture of the 3 mL nitric acid and 1 mL phosphoric acid was used for digestion in microwave equipment (Uniclever BMI-Z, Plazmatronika, Poland). The decomposed samples were transferred into 50 mL volumetric flasks, and the sample solutions were 10 times diluted before the analysis. Isotopes ^{59}Co, ^{57}Fe and ^{66}Zn were monitored for cobalt, iron and zinc, respectively. Calibration solutions of the determined elements and the internal standard (Rh) solution were prepared by dilution of the solutions of concentration 1.000±0.002 g/L (Merck, Darmstadt, SRN, Germany). The solutions were acidified by nitric acid (Suprapur; Merck) (5 mL/100 mL), and demineralized water (Milli-Q; Millipore, Billerica, MA, USA) was added. Measurements of ICP-MS were performed on a spectrometer Elan DRC-e (Perkin Elmer, Concord, ON, Canada) equipped with a concentric nebulizer with a cyclonic cloud chamber and reaction/collision cell to eliminate interferences and with a peristaltic Gilson 212 pump.

MR relaxometry and imaging

Suspensions of iPSC-NPs labeled with different concentrations (5, 10 and 15 μg Fe/mL of cultured media) with two types of nanoparticles (CZF and PLL-coated γ-Fe_2O_3) for 72 hours were washed three times with PBS or transferred to differentiating medium for 1 week. The effect of nanoparticles on image contrast can be estimated from the relaxivities of the labeled cells. We also measured the suspensions of nanoparticles without cells in 4% gel phantoms. T_2 relaxation time of the 4% gel phantoms containing the cells was measured on a Bruker Minispec MQ20 relaxometer (Bruker, Germany; 20 MHz, 21°C) using a CPMG sequence with these parameters: 5 s recycle delay, 1 ms interpulse delay, eight scans and 3,000 points for fitting. Relaxivity r_2 was calculated as the inverse relaxation time T_2 after deducting the contribution of gel and unlabeled cells and related to the cell concentration of the measured sample. T_2-weighted images of the 4% gel phantoms containing homogenously distributed cells were acquired on a 4.7 T Bruker Biospec scanner using a commercial resonator coil

(Bruker, Biospin, Germany). A standard two-dimensional rapid acquisition with relaxation enhancement multispin echo sequence was used with the following parameters: repetition time =3,000 ms, echo time =14 ms, spatial resolution =137×137 μm^2, slice thickness =0.5 mm, number of acquisitions =1 and acquisition time =9 min 36 s.

Flow cytometry analysis

Non-differentiating or differentiating iPSC-NPs were dissociated from monolayers by trypsin (Gibco) for 2 min. After rinsing with PBS (Gibco), the cell suspension (10^7 cells/mL and no less than 5×10^5 cells per sample) was used for flow cytometric analysis using a Becton Dickinson FACSAria flow cytometer (BD Biosciences, San Diego, CA, USA). Data analysis was performed using BD FACSDiVa software. To analyze the human iPSC-NPs, conjugated antibodies against CD15 (SSEA-1)/PerCP, CD24/FITC, CD29/APC, CD44/FITC, CD56 (NCAM)/APC or PE, CD271 (NGFR)/PE (Exbio Antibodies, Vestec u Prahy, Czech Republic), Ki67/FITC, sox2/APC (BD Pharmingen, San Diego, CA, USA), SSEA4/PE (BioLegend, San Diego, CA, USA), nanog/FITC, oct3/4/APC, TRA-1-60/PE, CD184/PE (eBioscience, San Diego, CA, USA), A2B5/APC, CD133/PE (Miltenyi Biotec, Bergisch Gladbach, Germany) and β-III-tubulin/FITC (BD Biosciences) were used. Unconjugated mouse nestin and rabbit neurofilament 70 (NF70) (Abcam, Cambridge, UK) were labeled with secondary rat anti-mouse IgG FITC (eBioscience) and secondary donkey anti-rabbit APC, respectively (Jackson Immunoresearch Laboratories, West Grove, PA, USA). As negative controls, mouse IgG1 isotype conjugated with FITC or RPE and IgG2a isotype conjugated with RPE (Dako Cytomation, Glostrup, Denmark) and secondary antibodies without the addition of the primary antibody were used. Briefly, cells were sampled in designed tubes, at least 250,000 cells in 100 μL, and incubated with an appropriate amount of antibodies according to the manufacturer's recommendation. For intracellular staining, cells were first fixed with 4% paraformaldehyde and permeabilized with 1× BD Perm/Wash Buffer (BD Pharmingen). Cells were washed with PBS, and at least 10,000 cells were recorded on BD FACSAria™ Cell Sorter (BD Biosciences) equipped with 488 and 633 nm lasers. Acquired data were analyzed using BD FACSDiVa Software (BD Biosciences).

RNA extraction and quantitative polymerase chain reaction (qPCR) analysis of gene expression

Total RNA was extracted from human iPSC-NPs (before and 2 weeks after the onset of differentiation) using the RNeasy Plus Mini Kit (catalog no 74134) from QIAGEN GmbH (Hilden, Germany), according to the manufacturer's instructions. cDNA was transcribed with a Transcriptor Universal cDNA Master (catalog no 05893151001; Roche), according to the manufacturer's instructions. The expressions of human (*Homo sapiens*) target genes *NES*, *TUBB3*, *GFAP*, *GAPDH*, *TH*, *SYP*, *EN1*, *NR4A2* and *FOXA2* were determined by quantitative real-time reverse transcription qRT-PCR in a StepOne™ Real-Time PCR Systems (Applied Biosystems, Foster City, CA, USA) using a TaqMan Gene Expression Master Mix (catalog no 4392938) and TaqMan Gene Expression Assays 4331182.

Hs00707120_s1/NES/, Hs00801390_s1/TUBB3/, Hs00909233_m1/GFAP/, Hs99999905_m1/GAPDH/, Hs00165941_m1/TH/, Hs00300531_m1/SYP/, Hs00154977_m1/EN1/, Hs00428691_m1/NR4A2/, Hs00232764_m1/FOXA2/.

The qPCR was carried out in a final volume of 20 μL containing 500 ng of extracted RNA. The following thermal profile was used: a single cycle of RT for 10 min at 55°C and 5 min at 85°C for reverse transcriptase inactivation and DNA polymerase activation, followed by 40 cycles of denaturation at 95°C for 15 s and annealing and extension at 60°C for 1 min. The results were analyzed using integrated StepOne™ Software (version 2.3). Normalization of all data was achieved against glyceraldehyde 3-phosphate dehydrogenase (GAPDH), and data were transformed to a log 2 scale. Gene expression data in differentiating cells are presented relative to the average expression in the unlabeled undifferentiated control. All numerical data are presented as a mean of the logarithmic ratio from three independent experiments ± standard error of the mean. Statistical analyses of the differences in gene expression between samples were evaluated using one-way analysis of variance. Values of $P<0.05$ were considered significant.

Immunocytochemistry

Cells were washed in PBS (10 mM) and fixed in 4% paraformaldehyde in PBS for 30 min. Prior to immunostaining, the fixed cells were washed three times in PBS and permeabilized with 0.3% solution of Tween 20 for 20 min. The cells were treated for 2 hours at room temperature with 10% ChemiBLOCKER™ (2170; Millipore) and 0.1% solution Tween 20 in PBS to block nonspecific staining. To identify undifferentiated iPSC-NPs and differentiated neurons, antibodies against nestin (mouse monoclonal IgG1, MAB5326; Merck-Millipore, Billerica, MA, USA; 1:100); β-III-tubulin (Tuj 1, rabbit polyclonal, T3952; Sigma-Aldrich; 1:200); neurofilament 160 kDa (NF160, mouse monoclonal IgG1,

N-5264; Sigma-Aldrich; 1:200); tyrosine 3-hydroxylase (rabbit polyclonal antibody, ab137869; Merck-Millipore; 1:1,000); glial fibrillary acidic protein (GFAP, mouse monoclonal IgG1 conjugated with Cy3, C-9205; Sigma-Aldrich; 1:800); synaptophysin (mouse monoclonal IgG1, MAB5258; Merck-Millipore; 1:1,000) and doublecortin (DCX, goat polyclonal IgG, sc-8066, Santa Cruz, Heidelberg, Germany; 1:500).

To visualize primary antibody reactivity, appropriate secondary antibodies were used: goat anti-rabbit IgG (H+L) antibody conjugated with alexa fluor 488 (A-11008; Thermo Scientific, Rockford, IL, USA; 1:200), goat anti-mouse IgG (H+L) antibody conjugated with alexa fluor 488 (A-11029; Thermo Scientific; 1:200) and donkey anti-goat IgG (H+L) antibody conjugated with alexa fluor 488 (A-11055; Thermo Scientific; 1:400). Each secondary antibody was diluted in 0.1 M PBS with Chemiblocker (10%) and Tween 20 (0.1%) for 2 hours at room temperature. Additional nucleic acid staining was performed with 4′,6-diamidino-2-phenylindole, dihydrochloride (DAPI, D1306; Life Technologies, Carlsbad, CA, USA; 1:1,000). After immunostaining, the coverslips with cells were mounted using Aqua-Poly/Mount (18606-20; Polysciences Inc., Warrington, PA, USA). Confocal images were taken with a Zeiss LSM 5 Duo confocal microscope (Carl Zeiss AG, Oberkochen, Germany). To visualize the nanoparticles in differentiating cells, brightfield and immunofluorescence images were combined. To estimate the number of NF160-positive cells, at least 650 cells per group within randomly selected fields were analyzed using ImageJ (National Institutes of Health).

Results

Nanoparticles uptake, detection and quantification

Intracellular labeling efficiency was determined after 72 hours of iPSC-NPs cultivation with different concentrations of CZF and PLL-coated γ-Fe_2O_3. PLL-coated γ-Fe_2O_3 were more efficient than CZF (82.7%±3.5% and 71.6%±5.1%, respectively). However, only in the lowest concentration (5 μg Fe/mL) was the difference between two types of nanoparticles significant (Figure 1A). Figure 1B shows a representative picture of magnetically labeled cells after 72 hours. Iron was visualized as blue granules by PB staining only in cells labeled with PLL-coated γ-Fe_2O_3. In CZF-labeled cells, the brown granules correspond to the nanoparticles as CZF have a silica coating, which does not allow the staining for iron. Images show no presence of granules in unlabeled cells, and the increased labeling efficiency corresponds to the higher nanoparticle concentration in both CZF- and PLL-coated γ-Fe_2O_3-labeled cells. Internalization of nanoparticles was confirmed using TEM images in labeled cells before and during differentiation. Differentiating cells possess tinier cell bodies in comparison to undifferentiated cells and prominent neurofilaments corresponding to developing processes. Nanoparticles were observed as clusters inside the endosome or lysosome in the cytoplasm of undifferentiated and differentiating cells labeled with both CZF and PLL-coated γ-Fe_2O_3 (Figure 2). Chemical analysis of iron, cobalt and zinc content by ICP-MS revealed a higher intracellular concentration of iron in cells incubated with PLL-coated γ-Fe_2O_3 when compared to cells labeled with the same concentrations of CZF. ICP-MS showed that the average iron content was 3.21, 2.24 and 2.82 pg Fe/cell for different labeling concentrations (5, 10 and 15 μg Fe/mL) of CZF and 7.57, 18.04 and 22.63 pg Fe/cell for 5, 10 and 15 μg Fe/mL of PLL-coated γ-Fe_2O_3. A small amount of iron (0.13 pg Fe/cell) was detected in unlabeled cells. The concentration of iron increased in dependence on the concentration of PLL-coated γ-Fe_2O_3 in the cultivation medium. The concentration of iron did not change much in cells labeled with different concentrations of CZF. This also applies to the cobalt and zinc content. The data are summarized in Table 1.

To test the visualization of magnetically labeled cells using MR imaging, different concentrations of nanoparticles alone or iPSC-NPs labeled for 72 hours with different doses of CZF and PLL-coated γ-Fe_2O_3 were immobilized in 4% gelatin phantom and measured using MR. Relaxometry of both types of nanoparticles were comparable (Table 2). On the other hand, relaxometry revealed approximately twice higher r_2 values in PLL-coated γ-Fe_2O_3-labeled cells in comparison with CZF-labeled cells. The relaxivity values of labeled cells decreased during differentiation (Table 3). Relaxometry data correlated well with MR imaging of gel phantoms (Figure 3). The decrease of signal intensity in phantoms containing magnetically labeled cells corresponded to the presence of metallic ions in cells and was dependent on the concentration the cells were labeled with. Hypointense areas were more abundant in phantoms containing cells labeled with PLL-coated γ-Fe_2O_3 than with CZF and in undifferentiated cells than in differentiating cells (Figure 3).

Cell proliferation and differentiation

Cell proliferation was repeatedly analyzed in iPSC-NPs exposed to increasing concentrations of CZF and PLL-coated γ-Fe_2O_3 using the XCelligence system for 72 hours. CZF and PLL-coated γ-Fe_2O_3 contrast agents differed in their effect on cell proliferation. CZF significantly decreased cell growth in the first hours of incubation independent of concentration.

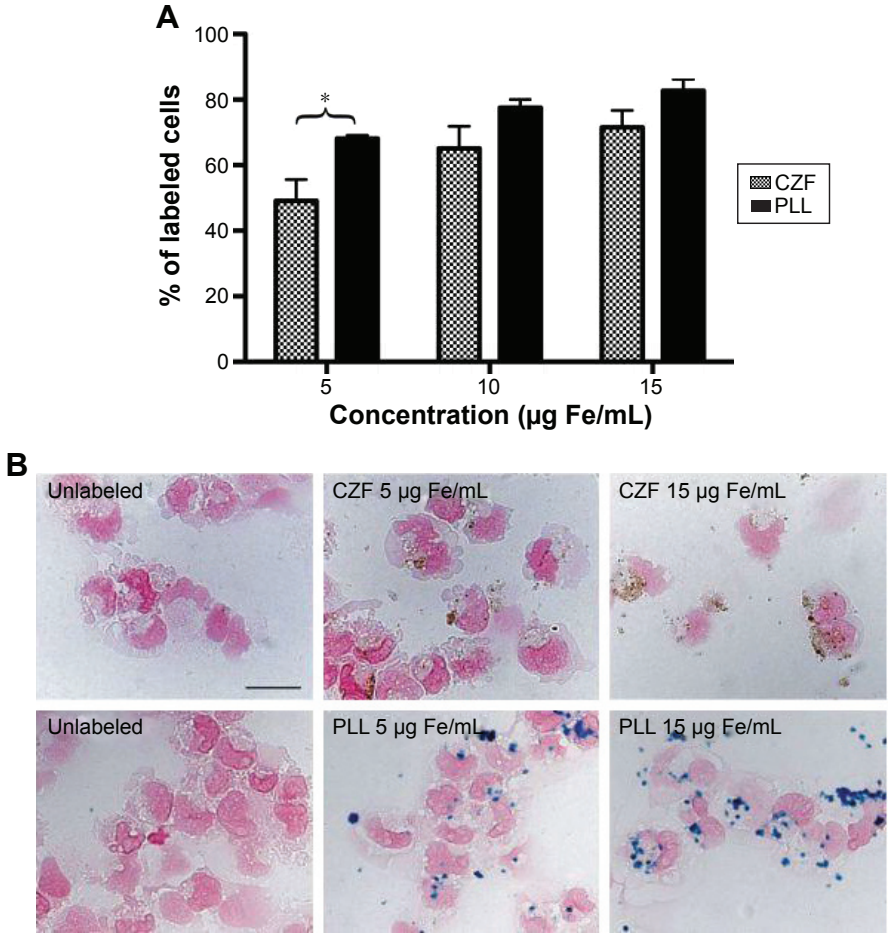

Figure 1 Labeling efficiency.
Notes: (**A**) Number of labeled iPSC-NP cells expressed as a percentage of total cell number counted after 72 hours cell growth with different concentrations of CZF and PLL-coated γ-Fe_2O_3 nanoparticles. The graph represents results from three independent experiments ± SD (*$P<0.05$). (**B**) Representative pictures of PB staining in iPSC-NPs treated with 5 and 15 µg Fe/mL for 72 hours show increasing labeling efficiency. Iron labeling was not present in unlabeled control. The bar represents 20 µm.
Abbreviations: iPSC-NPs, induced pluripotent stem cell-derived neural precursors; CZF, silica-coated cobalt zinc ferrite nanoparticles; PLL-coated γ-Fe_2O_3, poly-L-lysine-coated iron oxide superparamagnetic nanoparticles; PB, Prussian blue; SD, standard deviation.

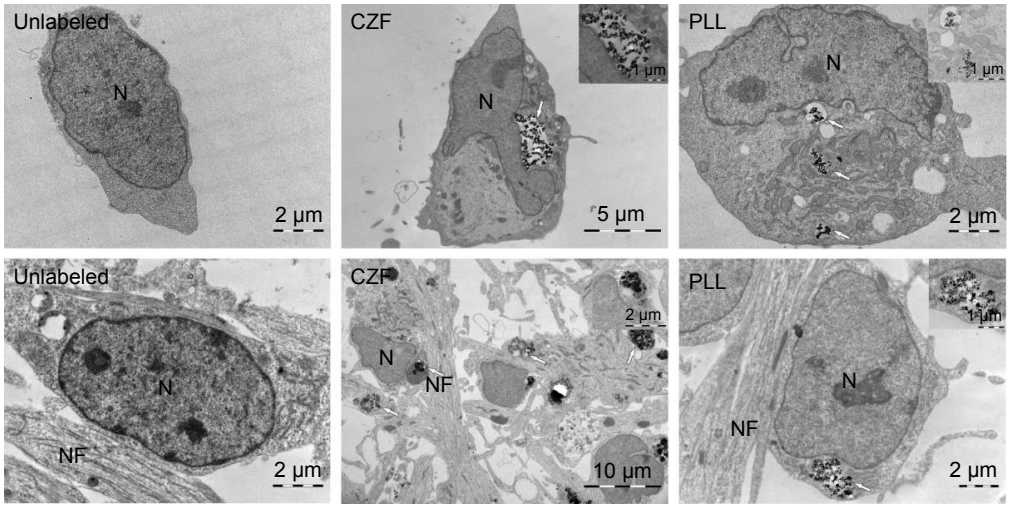

Figure 2 TEM confirmation of nanoparticles internalization.
Notes: Top row: undifferentiated cells unlabeled and labeled with 15 µg Fe/mL CZF and PLL-coated γ-Fe_2O_3 (PLL) for 72 hours. Bottom row: differentiating cells unlabeled and labeled with 15 µg Fe/mL CZF and PLL-coated γ-Fe_2O_3 (PLL) for 72 hours. Insets show higher magnification views of nanoparticle clusters surrounded by membrane. Nanoparticle clusters are marked by arrows.
Abbreviations: TEM, transmission electron microscopy; CZF, silica-coated cobalt zinc ferrite nanoparticles; PLL-coated γ-Fe_2O_3, poly-L-lysine-coated iron oxide superparamagnetic nanoparticles; N, nucleus; NF, neurofilaments.

Table 1 ICP-MS measurement

Nanoparticles	Cobalt (pg/cell)	Zinc (pg/cell)	Iron (pg/cell)
Unlabeled control	0.00	0.13±0.18	0.13±0.18
PLL-coated γ-Fe_2O_3 5 μg Fe/mL	–	–	7.57±1.90
PLL-coated γ-Fe_2O_3 10 μg Fe/mL	–	–	18.04±5.26
PLL-coated γ-Fe_2O_3 15 μg Fe/mL	–	–	30.23±10.93
CZF 5 μg Fe/mL	0.93±0.45	0.88±0.83	3.21±1.49
CZF 10 μg Fe/mL	0.61±0.10	0.69±0.02	2.24±0.43
CZF 15 μg Fe/mL	0.71±0.14	0.79±0.02	2.82±0.87

Notes: Iron, cobalt and zinc content in unlabeled control iPSC-NP cells and in cells labeled with different concentrations of CZF and PLL-coated γ-Fe_2O_3 (5, 10 and 15 μg Fe/mL for 72 hours) measured by ICP-MS (n=3). Mean ± SD.
Abbreviations: ICP-MS, inductively coupled plasma mass spectrometry; PLL-coated γ-Fe_2O_3, poly-L-lysine-coated iron oxide superparamagnetic nanoparticles; CZF, silica-coated cobalt zinc ferrite nanoparticles.

The significant negative effect on cell proliferation was constant in incubation longer than 40 hours with the highest dose (15 μg Fe/mL) (Figure 4A). In comparison, PLL-coated γ-Fe_2O_3 did not have any significant negative effect on cell proliferation in any dose (Figure 4B).

To analyze and quantify the expression of several pluripotent and neuroectodermal markers in differentiating unlabeled and labeled cells, single-cell suspensions were labeled with antibodies directed against Nanog, SSEA-4, SSEA-1, TRA-1-60, oct 3/4, sox2, CD44, CD133, A2B5, β-III-tubulin, NF70, nestin and Ki67. The expression profiles were categorized as follows, based on the percentage of positive cells: 0%–5% negative, 6%–39% low, 40%–79% moderate and 80%–100% high. Data are summarized in Table 4. The pluripotent markers Nanog, SSEA-4 and TRA-1-60 were negative in both undifferentiated and differentiating cells (labeled and unlabeled). Another pluripotent marker oct 3/4 was expressed in low levels before and during differentiation. During differentiation, the cytometry results revealed a decrease in the expression of the early progenitor markers sox2, CD133, CD15 and proliferative marker Ki67. The expression of the neuron-specific marker β-III-tubulin increased. In immunocytochemical analysis, we also did not observe any major difference between unlabeled and labeled cells in the differentiating pattern or the presence of the observed marker.

Table 2 Relaxivity r_2 in vitro of nanoparticles

r_2 ± SD (s^{-1})			
Nanoparticles	**5 μg Fe/mL**	**10 μg Fe/mL**	**15 μg Fe/mL**
CZF	7.22±0.07	7.91±0.21	16.75±0.21
PLL-coated γ-Fe_2O_3	6.52±0.24	11.48±0.05	17.63±0.04

Note: Relaxivity r_2 of different concentrations of CZF and PLL-coated γ-Fe_2O_3 without cells was measured in gel phantoms.
Abbreviations: CZF, silica-coated cobalt zinc ferrite nanoparticles; PLL-coated γ-Fe_2O_3, poly-L-lysine-coated iron oxide superparamagnetic nanoparticles; SD, standard deviation.

During differentiation, neural progenitors formed rossettes (not shown). After 2 weeks of differentiation, the majority of NPs showed the morphology of immature neurons, a spherical cell body with long processes. The majority of cells with this morphology were positive for β-III-tubulin. Fiber bundles were further positive for high-molecular-weight neurofilaments; the fluorescent signal of NF160 was present in ~87% of unlabeled cells, ~72% of CZF-labeled cells and ~70% of PLL-coated γ-Fe_2O_3-labeled cells (Figure 5). GFAP was present in a small fraction of the cells (Figure 5). Cells were also positive for the microtubule-associated protein doublecortin, a marker of immature neurons and synaptophysin. A marker of DA neurons, tyrosine hydroxylase, was present in <8% of the cells. These cells had the morphology of terminally differentiated neurons (Figure 6). The presence of nanoparticles in differentiating cells was confirmed on bright field images and their overlay with immunohistochemical staining of neuronal and astrocyte markers (Figure 7). The expression of selected genes was measured after 2 weeks of differentiation in unlabeled cells and cells labeled with CZF and PLL-coated γ-Fe_2O_3. Data were normalized to the average expression levels in undifferentiated unlabeled cells. The qPCR analysis revealed changes in the expression of neural markers during differentiation. The neural stem cell marker nestin was downregulated during differentiation in both unlabeled and labeled cells (Figure 8A). GFAP showed a significant increase in gene expression. Neuronal specific markers such as β-III-tubulin and synaptophysin were upregulated in differentiating cells labeled with PLL-coated γ-Fe_2O_3 (Figure 8A). Transcription factors involved in DA neurons development, EN1 and Nurr1, were upregulated significantly in unlabeled and labeled cells. FOXA2 was upregulated significantly in unlabeled cells and cells labeled with PLL-coated γ-Fe_2O_3, but mostly unchanged in CZF-labeled cells (Figure 8B). Enzyme TH, which hydroxylates tyrosine to levodopa, was upregulated significantly in both unlabeled and labeled cells.

Discussion

Magnetic labeling

In future of using labeled cells for clinical application in CNS diseases, it is crucial to ensure sufficient labeling to reliably monitor cells using MR. On the other hand, it is essential to preserve and not to violate any biological functions of the labeled cells or cause toxicity or affect unique stem cell characteristics: stemness and differentiation potential.[16] In this study, we tested two types of contrast agent: poly (L-lysine)-modified iron oxide and CZF. PLL-coated γ-Fe_2O_3 were already tested in rat bone marrow stromal cells (rMSCs)

Table 3 Relaxivity r_2 in vitro of labeled cells

r_2 [s^{-1}/mil cells/mL] ± SD				
Nanoparticles	**5 μg Fe/mL**	**10 μg Fe/mL**	**15 μg Fe/mL**	**1-week differentiation**
CZF	0.585±0.182	0.788±0.079	1.230±0.013	0.158±0.012
PLL-coated γ-Fe_2O_3	0.965±0.139	1.50±0.098	3.316±0.824	0.128±0.002

Notes: r_2 was measured in iPSC-NPs labeled with different concentrations of CZF and PLL-coated γ-Fe_2O_3 for 72 hours and homogenously suspended in gel phantoms. The table represents results from three independent experiments ± SD. Relaxivity r_2 is related to 1×10^6 cells.
Abbreviations: CZF, silica-coated cobalt zinc ferrite nanoparticles; PLL-coated γ-Fe_2O_3, poly-L-lysine-coated iron oxide superparamagnetic nanoparticles; SD, standard deviation.

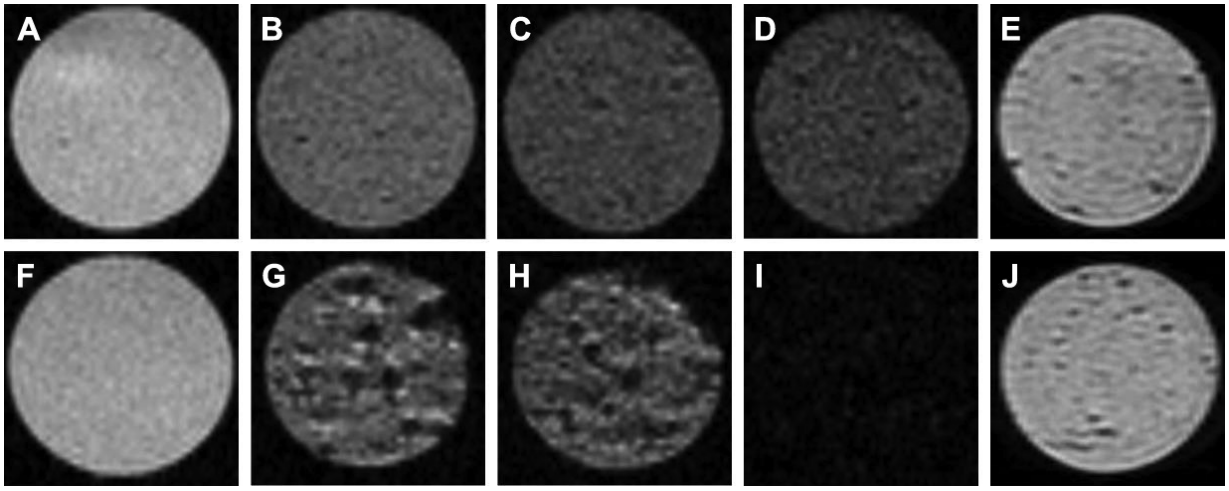

Figure 3 MR images of gel phantoms.
Notes: Gel phantoms without cells (**A**) and with unlabeled cells (**F**). Gel phantoms with iPSC-NPs labeled with different concentrations of CZF in culture medium for 72 hours: 5 μg Fe/mL (**B**); 10 μg Fe/mL (**C**); 15 μg Fe/mL (**D**) and 1 week after onset of differentiation (**E**). Gel phantoms with iPSC-NPs labeled with PLL-coated γ-Fe_2O_3 at concentrations of 5 μg Fe/mL (**G**); 10 μg Fe/mL (**H**); 15 μg Fe/mL (**I**); and 1 week after onset of differentiation (**J**). Signal decrease and hypointense spots in phantoms correspond to the amount of metallic ions in cells.
Abbreviations: MR, magnetic resonance; iPSC-NPs, induced pluripotent stem cells-derived neural precursors; CZF, silica-coated cobalt zinc ferrite nanoparticles; PLL-coated γ-Fe_2O_3, poly-L-lysine-coated iron oxide superparamagnetic nanoparticles.

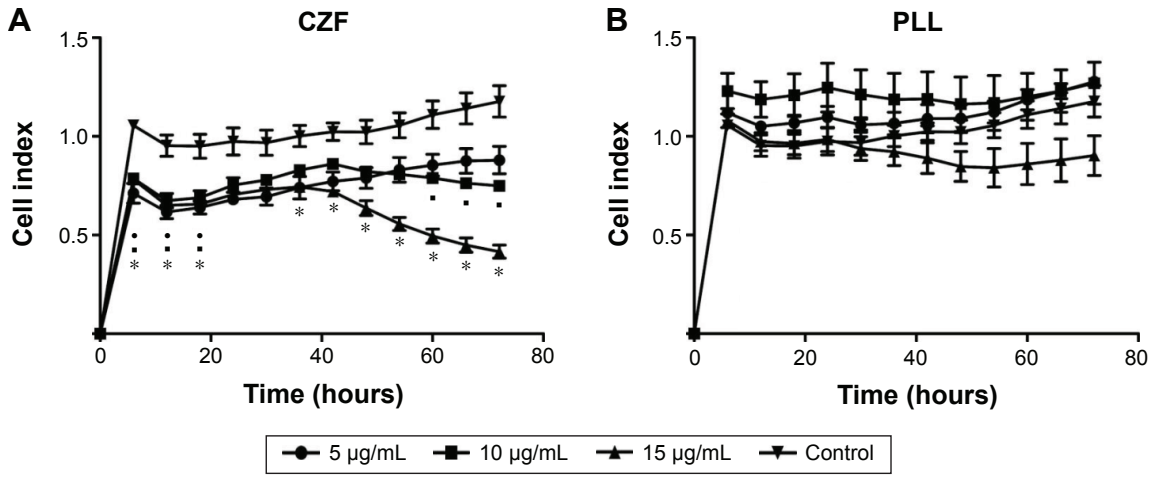

Figure 4 Time-dependent proliferation profile of unlabeled control and labeled iPSC-NP cells.
Notes: Proliferation curves of cells labeled with different concentrations of CZF and unlabeled control (**A**) and with PLL-coated γ-Fe_2O_3 and unlabeled control (**B**). Cell index represents cell viability, number, morphology and adhesion degree. Graphs represent results from three independent experiments ± SD ($P<0.05$; ● corresponds to difference between 5 μg Fe/mL and control; ■ corresponds to difference between 10 μg Fe/mL and control; * corresponds to difference between 15 μg Fe/mL and control).
Abbreviations: iPSC-NP, induced pluripotent stem cell-derived neural precursors; CZF, silica-coated cobalt zinc ferrite nanoparticles; PLL-coated γ-Fe_2O_3, poly-L-lysine-coated iron oxide superparamagnetic nanoparticles; SD, standard deviation.

Table 4 Changes in markers expression during iPSC-NPs differentiation detected using flow cytometry

Marker	Undifferentiated unlabeled cells	Differentiated unlabeled cells	Differentiated cells labeled with CZF	Differentiated cells labeled with PLL-coated γ-Fe_2O_3
Nanog	–	–	–	–
SSEA-4	–	–	–	–
TRA-1-60	–	–	–	–
Oct 3/4	+	+	+	+
Sox2	++	+	+	+
CD133	+++	+	+	+
SSEA-1 (CD15)	+++	++	++	++
CD44	+	–	+	+
A2B5	+	+	+	+
NF70	++	+	+	++
Nestin	++	++	++	++
β-III-Tubulin	+	++	+++	++
Ki67	+++	++	++	++

Notes: Comparative analysis of the expression of pluripotent and neural markers in unlabeled control and cells labeled with CZF or PLL-coated γ-Fe_2O_3 (15 μg Fe/mL in cultivation media for 72 hours) in undifferentiated and differentiating cells. All results are expressed as percentages of the whole population: 0%–5%, negative (–); 6%–39%, low level of marker expression (+); 40%–79%, moderate level of marker expression (++); 80%–100%, high level of marker expression (+++).

Abbreviations: iPSC-NPs, induced pluripotent stem cell-derived neural precursors; CZF, silica-coated cobalt zinc ferrite; PLL-coated γ-Fe_2O_3, poly-L-lysine-coated iron oxide superparamagnetic nanoparticles.

and human marrow stromal cells (hMSCs) in vitro and in vivo.[18,23,24] CZF were shown to have good electromagnetic performance and excellent chemical stability so they are promising candidates for biomedical application.[25] However, their biological effect has not been studied in much detail. They were tested in vitro with silica coating in rMSCs[22] and in human prostate cancer cell lines (DU145 and PC3) with biocompatible dimercaptosuccinic acid (DMSA) coating.[26,27] Our results show that PLL-coated γ-Fe_2O_3 slightly slowed down cell proliferation of iPSC-NPs only in the highest concentration (15 μg Fe/mL). In the previous experiments, the cultivation of hMSCs with PLL-coated γ-Fe_2O_3 in the same concentration also resulted in a slight reduction of cell viability according to WST colorimetric assay. However, this effect was reversible after 72 hours incubation in SPION-free medium.[24] CZF slowed down iPSC-NPs proliferation especially in higher concentrations (15 μg Fe/mL). In comparison, these nanoparticles did not have any effect on the cell proliferation of rMSCs in similar concentrations.[22] In vitro cell viability of PC3 after 24-hour exposure to CZF coated with DMSA assessed by MTT assay did not decrease compared to the control group up to a concentration of 0.9 mM, which could correspond with shorter incubation time in comparison with our experiments. In higher concentrations than 0.9 mM CZF, the viability of PC3 was <50%.[26] Human iPSC-NPs seem to be more sensitive to CZF labeling than rMSCs and PC3 even in lower doses.

The labeling efficiency in our experiments increased with higher concentrations of iron in the cultivation medium. CZF were nonsignificantly less efficient in labeling the iPSC-NPs (72%) in comparison with PLL-coated γ-Fe_2O_3 (82%). Similar labeling efficiency was found in PLL-coated γ-Fe_2O_3-labeled hMSCs and rMSCs.[23,24] Comparable labeling efficiencies were shown in the labeling of neural stem cells with various types of contrast agents.[28–31] Further, we confirmed the internalization of both types of contrast agents in cell cytoplasm using TEM. Nanoparticles were present in cytoplasm in clusters surrounded by a membrane. The intracellular content of iron in iPSC-NPs in the highest dose reached 22.63 pg Fe/cell for PLL-coated γ-Fe_2O_3. The intracellular iron content in iPSC-NPs labeled with CZF (2.82 pg Fe/cell) is similar to previously reported results from NSCs labeling.[30,32] The iron content in iPSC-NPs is sufficient for MR imaging as 1.4–3.0 pg Fe/cell was assessed as a minimum concentration required for detection with MR imaging in the case of SPIONs.[33] Besides iron content in the cell and the labeling efficiency, an essential characteristic for cell detection on MR is the relaxivity of the contrast agent itself, as the relaxation times affect the contrast enhancement in T_1-, T_2- and T_{2*}-weighted images.[34] The relaxivity properties depend on the nanoparticles used and are affected by their surface modification. In our results, the relaxivities of both nanoparticles in gel phantoms were comparable and dependent on concentration. The relaxivities of labeled cells were proportional to increasing concentrations of nanoparticles during cell labeling; PLL-coated γ-Fe_2O_3-labeled cells reached approximately double relaxivity rates than cells labeled with CZF, which corresponds to higher

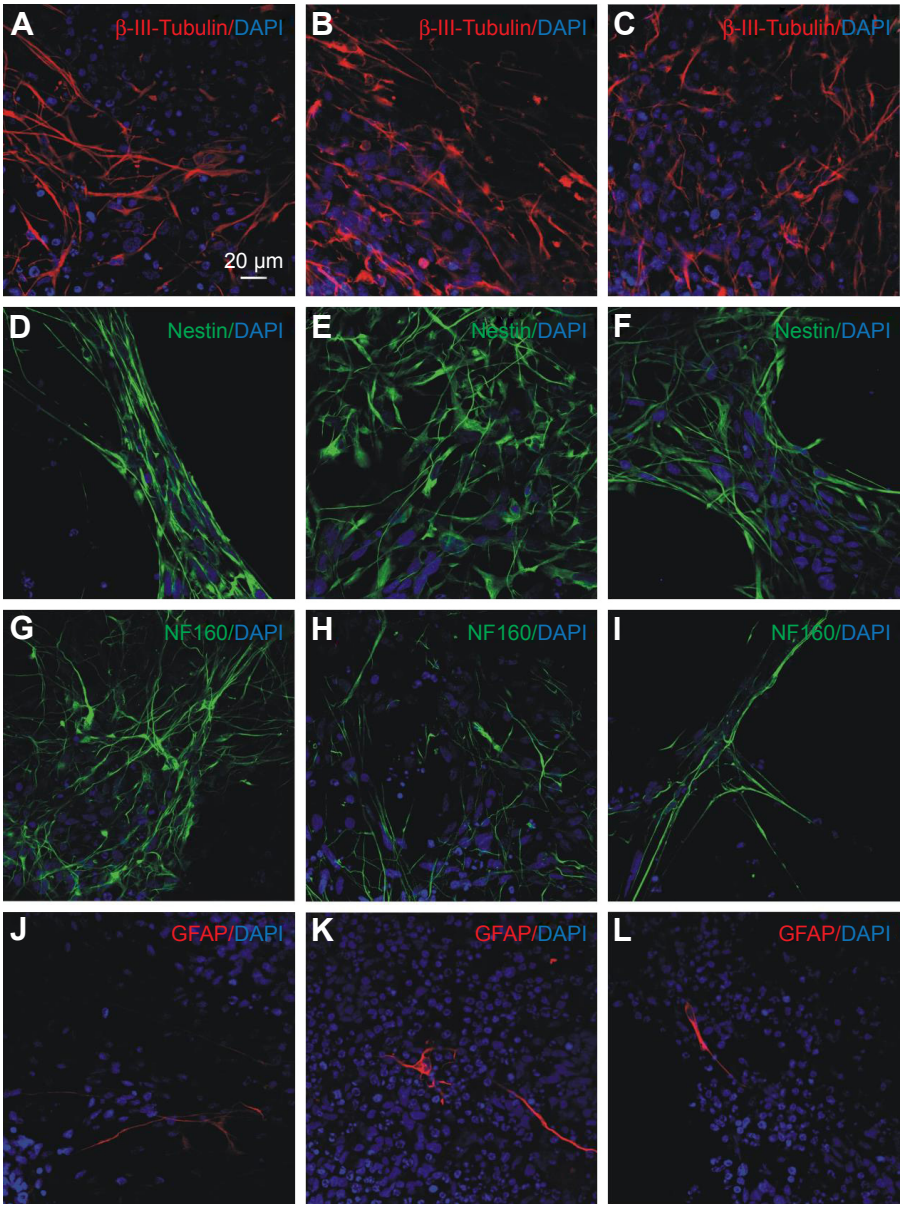

Figure 5 Immunocytochemical characterization of differentiating iPSC-NPs.

Notes: First column (**A**, **D**, **G** and **J**) represents unlabeled cells, second column (**B**, **E**, **H** and **K**) represents cells labeled with CZF (15 μg Fe/mL in cultivation media for 72 hours), and third column (**C**, **F**, **I** and **L**) represents cells labeled with PLL-coated γ-Fe_2O_3 (15 μg Fe/mL in cultivation media for 72 hours). Cells are stained for β-III-tubulin (**A**–**C**) red, nestin (**D**–**F**), NF160 (**G**–**I**) green, GFAP (**J**–**L**) red and DAPI (blue) 2 weeks after onset of differentiation.

Abbreviations: iPSC-NPs, induced pluripotent stem cell-derived neural precursors; CZF, silica-coated cobalt zinc ferrite nanoparticles; PLL-coated γ-Fe_2O_3, poly-L-lysine-coated iron oxide superparamagnetic nanoparticles; NF160, neurofilament 160 kDa; GFAP, glial fibrillary acidic protein; DAPI, 4′,6-diamidino-2-phenylindole, dihydrochloride.

labeling efficiency and higher iron content in PLL-coated γ-Fe_2O_3-labeled cells. Generally, the relaxivities of labeled iPSC-NPs were lower than in labeled rMSCs or hMSCs, regardless of the type of nanoparticles.[22,23] While the percentage of labeled cells is comparable in MSCs and iPSC-NPs, MSCs tend to endocytose more nanoparticles, and the labeling is more intense (Turnovcova, unpublished data, 2014) than in neural precursor cells, using the same concentrations and the same labeling time. These results correspond to the significantly higher amount of iron per cell in magnetically labeled MSCs.[18,22] MR imaging of gel phantoms with labeled iPSC-NP cells reflects the labeling efficiency. The signal decreased more in PLL-coated γ-Fe_2O_3-labeled cells than in CZF-labeled cells and also when higher nanoparticle concentrations were used. However, we could easily detect cells in all samples, including differentiating cells, as hypointense spots. On the other hand, unlabeled cells showed the same signal intensity as gel-only phantoms, and therefore,

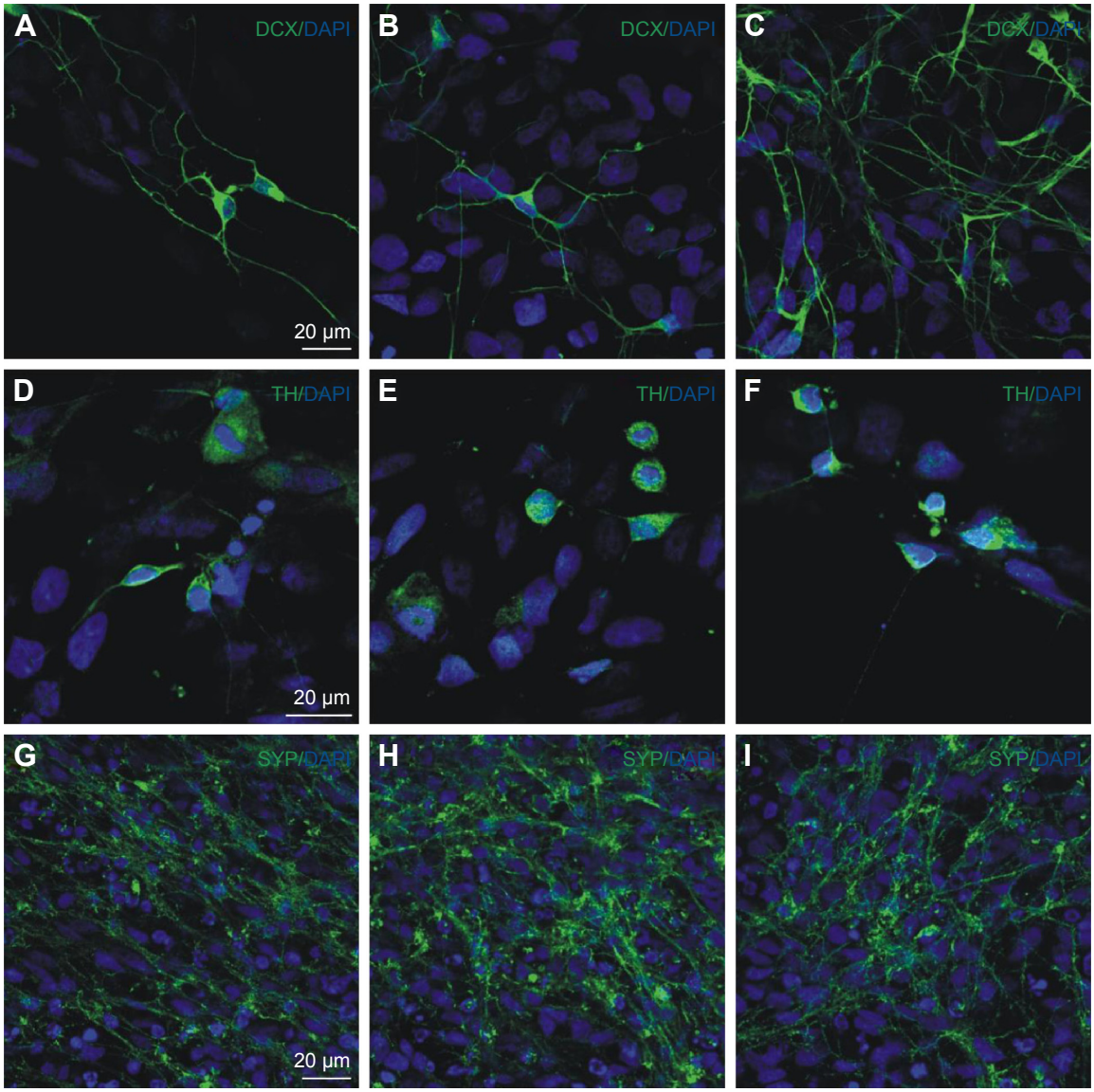

Figure 6 Immunocytochemical characterization of differentiating iPSC-NPs.
Notes: First column (**A**, **D**, **G**) represents unlabeled cells, second column (**B**, **E**, **H**) represents cells labeled with CZF (15 µg Fe/mL in cultivation media for 72 hours), and third column (**C**, **F**, **I**) represents cells labeled with PLL-coated γ-Fe_2O_3 (15 µg Fe/mL in cultivation media for 72 hours). Cells are stained for doublecortin (**A**–**C**), TH (**D**–**F**), synaptophysin (**G**–**I**) green and DAPI (blue).
Abbreviations: iPSC-NPs, induced pluripotent stem cell-derived neural precursors; CZF, silica-coated cobalt zinc ferrite nanoparticles; PLL-coated γ-Fe_2O_3, poly-L-lysine-coated iron oxide superparamagnetic nanoparticles; DCX, doublecortin; SYP, synaptophysin; DAPI, 4′,6-diamidino-2-phenylindole, dihydrochloride.

they were not detectable on MR imaging. The relaxivity rates decreased during differentiation, which might correspond to the cell proliferation and contrast dilution also reported in other labeling studies.[28,29,31] However, this could be overcome in in vivo experiments where following transplantation in the CNS, the majority of cells differentiate and diminish their replication potential[35,36] or exit the cell cycle and retain the intracellular SPIO over a longer time period.[28] This is in agreement with in vivo experiments of SPIO-labeled neural stem cells.[29,31,37] Results from cell labeling and MR support the idea that cell labeling of iPSC-NPs both with PLL-coated γ-Fe_2O_3 (SPION) and with CZF is sufficient to detect the cells in MR imaging in vivo. However, further experiments of in vivo models of PD will be necessary.

Cell differentiation

As mentioned earlier, the unique characteristics of pluripotent cells are their stemness and differentiation potential. IPSCs have the potential for studying and treating a wide range of neurological conditions, such as amyotrophic lateral sclerosis,[38] PD,[10] Alzheimer's disease[39] or multiple sclerosis.[40] The promise of stem cell-based therapy for

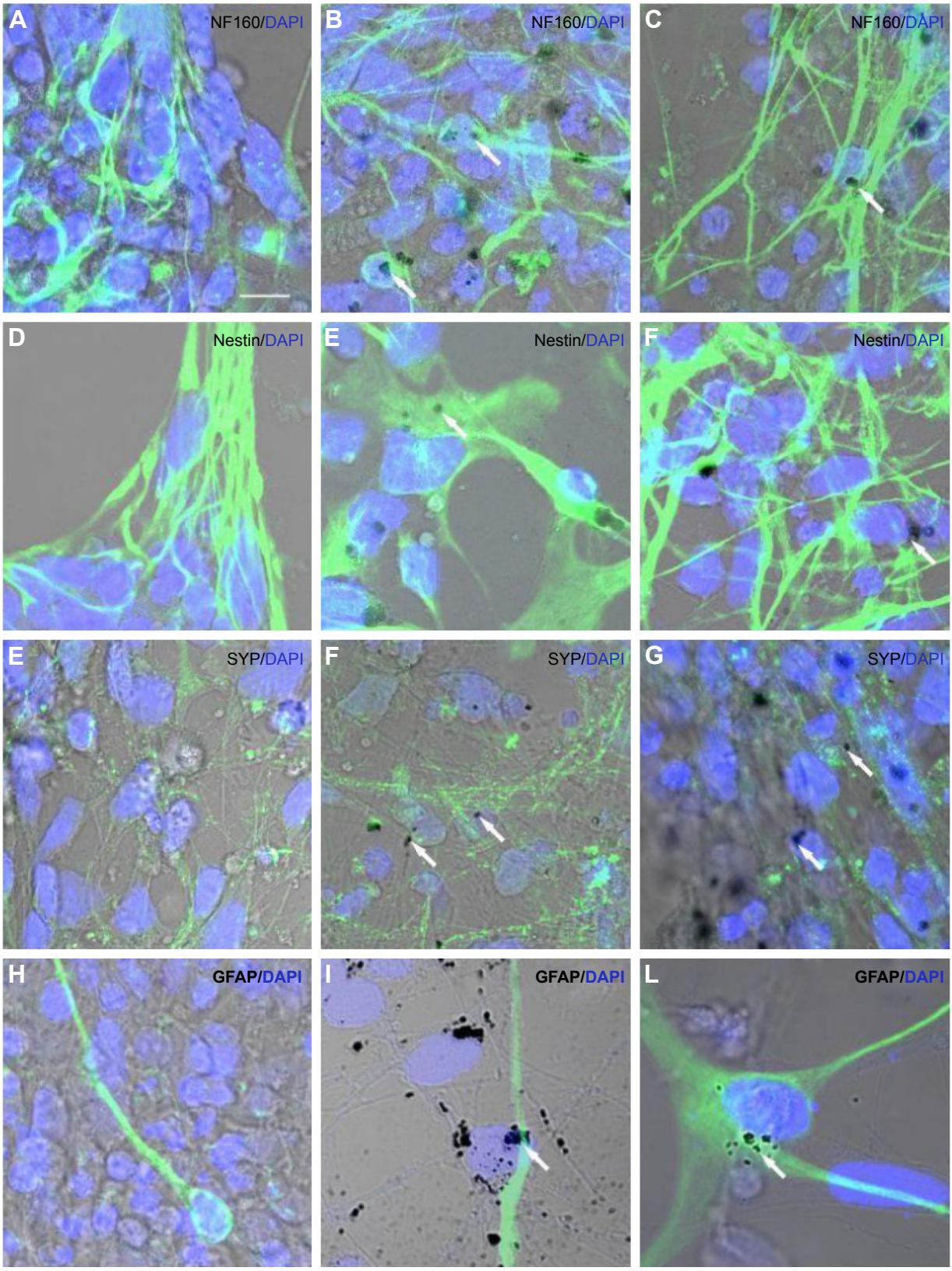

Figure 7 Nanoparticles in differentiating cells.

Notes: First column (**A**, **D**, **E**, **H**) represents unlabeled cells, second column (**B**, **E**, **F**, **I**) represents cells labeled with CZF, and third column (**C**, **F**, **G**, **J**) represents cells labeled with PLL-coated γ-Fe_2O_3. Cells are stained for NF160 (**A**–**C**), nestin (**D**–**F**), synaptophysin (**E**–**G**), GFAP (**H**–**J**) green and DAPI (blue). Nanoparticles are visualized as dark spots and are marked by arrows. The bar represents 10 μm.

Abbreviations: CZF, silica-coated cobalt zinc ferrite nanoparticles; PLL-coated γ-Fe_2O_3, poly-L-lysine-coated iron oxide superparamagnetic nanoparticles; NF160, neurofilament 160 kDa; SYP, synaptophysin; GFAP, glial fibrillary acidic protein; DAPI, 4′,6-diamidino-2-phenylindole, dihydrochloride.

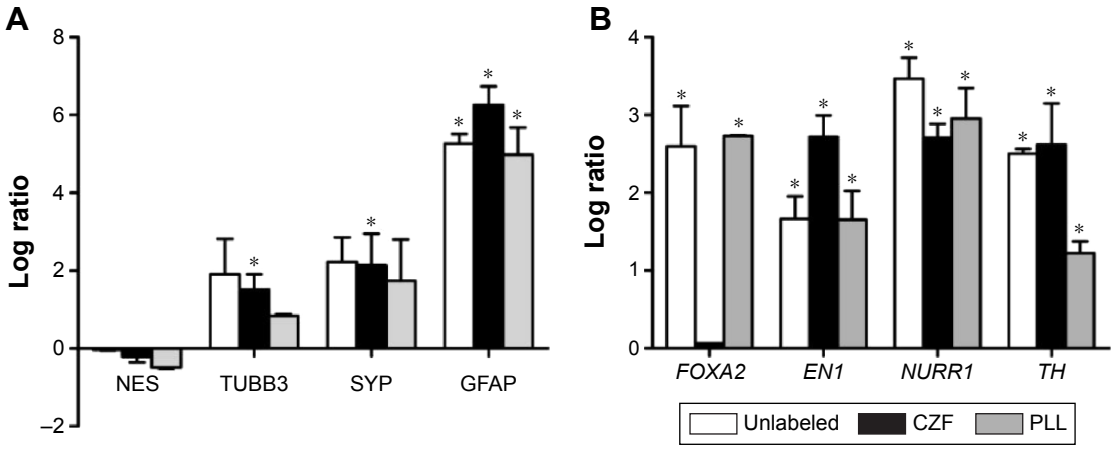

Figure 8 qRT-PCR analysis.

Notes: Unlabeled and labeled iPSC-NPs with CZF and PLL-coated γ-Fe_2O_3 were analyzed 2 weeks after the onset of differentiation. (**A**) The expression of the neural genes NES, TUBB3, SYP, and GFAP. (**B**) The expression of the mDN genes *FOXA2*, *EN1*, *NURR1* and *TH* (*$P<0.05$). The average expression of studied markers in the unlabeled undifferentiated control was set as zero.

Abbreviations: qRT-PCR, quantitative real-time reverse transcription polymerase chain reaction; iPSC-NPs, induced pluripotent stem cell-derived neural precursors; CZF, silica-coated cobalt zinc ferrite nanoparticles; PLL-coated γ-Fe_2O_3, poly-L-lysine-coated iron oxide superparamagnetic nanoparticles; SYP, synaptophysin; GFAP, glial fibrillary acidic protein; mDN, midbrain dopaminergic neuron.

neurodegenerative diseases is more relevant as 90% of new treatment compounds have failed in clinical trials.[41] In in vitro conditions, administration of factors involved in mammalian neurogenesis leads to the expression of specific transcription factors that regulate their differentiation into neurons and specific neuronal subtypes.[42] Even though the factors controlling neuronal differentiation are known, they are not easily controlled in vitro. The human iPSCs maintained in culture typically display heterogeneity, containing subset populations that express varying levels of pluripotency markers.[11] Neural precursors derived from iPSCs by dual inhibition of SMAD signaling,[9] which were used in this study, are stem cells committed to the neural cell lineage (neurons, astrocytes and oligodendrocytes). This reduces the risk of tumorigenesis present in pluripotent cells. The iPSC-NPs were differentiated to DA neurons and motoneurons in vitro.[9] To analyze the differentiation potential of labeled and unlabeled iPSC-NPs and quantify the presence of pluripotent neural and neuronal markers, we screened the cell population using flow cytometry, which enables rapid quantitative readout. The decrease in the positivity for stem cell markers nestin, NF70, SOX2, CD133 and CD15 and proliferative marker Ki 67 shows the differentiating pattern in the population. The expression profile corresponds to previous flow cytometry analysis of the same iPSC-NPs during pre-differentiation in vitro.[20,43] The presence of A2B5 and CD44 in differentiating cells confirms the heterogeneity of the differentiating population and is also in agreement with Romanyuk et al.[43] Increased expression of the neuronal marker β-III-tubulin during differentiation corresponds to our immunocytochemical data. The majority of differentiating cells were positive for β-III-tubulin and NF160. Cells changed morphology and formed projections, and the cell bodies were smaller revealing that cells became immature neurons. Among the differentiating population were cells with neuronal morphology positive for the DA neuronal marker TH and also for synaptophysin, a membrane glycoprotein essential to synapse formation, which shows that some cells were terminally differentiated. The reason for the small number of mature neurons and TH-positive cells among the differentiating culture in our study may be the slow maturation process of the human DA neurons in vitro.[4,44] Only a small portion (<2%) of the cells was GFAP-positive astrocytes. According to our results, TEM analysis confirms that nanoparticles were present inside the cytoplasm of differentiating cells. It is difficult to exactly quantify the number of magnetically labeled differentiating cells, since the nanoparticles themselves are not visible on immunohistochemical images, and only the overlay of bright field images with immunohistochemical staining can be used. Therefore, we quantified the differentiation process using flow cytometry, and in addition, we calculated the percentage of magnetically labeled cells expressing NF160, which is a typical neuronal marker. We did not observe any substantial differences in differentiation potential between labeled and non-labeled cells. This is in agreement with previous results on the differentiation of labeled cells in human ventral mesencephalic cells,[31] human fetal midbrain-derived neural precursor,[37] SPIO-labeled human neural stem cells[28] and human fetal neural precursor cells.[45] Similarly, in iPSC-derived neural stem cells, labeling of cells with various

contrast agents did not affect the differentiation potential into various types of neural precursor cells.[46] Our results from qRT-PCR analysis showed that the early neural marker nestin was downregulated and neuronal markers (β-III-tubulin and synaptophysin) were upregulated during the differentiation of iPSC-NPs.

The development of midbrain dopaminergic neurons (mDNs) is composed of a series of stages and orchestrated by cell intrinsic and extrinsic factors. EN1 is required for the generation of the midbrain–hindbrain junction and later for the maturation and survival of mDN.[47] FOXA 1/2 regulates multiple phases of mDN development.[48] NURR1 is a postmitotic marker of mDN preceding TH expression in the subventricular cell population.[47] The gene expression of transcription factors En1, Nurr1 and enzyme TH was upregulated in differentiating iPSC-NPs both in labeled and in unlabeled control. The gene expression of FOXA2 was affected in CZF-labeled cells. The FOXA2 transcription factor is biochemically connected with SHH,[47] which might suggest that CZF labeling might interfere with this pathway. The negative effect of CZF on cell differentiation should be considered in future experiments. The mDN markers were also upregulated in other studies aimed at in vitro differentiation of DA neurons from human iPSCs[4,44,49,50] or were detected immunocytochemically in differentiating cells.[6,44]

Conclusion

In this study, we demonstrated that iron-coated nanoparticles in low doses do not negatively affect iPSC-NP proliferation. However, neural precursors are more sensitive to incubation with CZF in comparison with PLL-coated γ-Fe_2O_3. The doses of nanoparticles and labeling time used were sufficient for MR detection, and they did not affect differentiation potential. The detection using MR suggests the suitability of PLL-coated γ-Fe_2O_3 for noninvasive cell tracking in future neural cell therapy-based in vivo applications for different disease models.

Acknowledgments

This work was supported by the Ministry of Education, Youth and Sports of CR within the LQ1604 National Sustainability Program II (Project BIOCEV-FAR) and by the project "BIOCEV" (CZ.1.05/1.1.00/02.0109), from the Norwegian Financial Mechanism 2009–2014 and the Ministry of Education, Youth and Sports under Project Contract no MSMT-28477/2014; project 7F14057 and MH CR-DRO (Institute for Clinical and Experimental Medicine IKEM, IN00023001). This paper was presented in part at the 10th Czech Neuroscience Society Meeting, November 18–19, 2015, as a poster presentation with interim findings. The actual paper, however, has never been published. Pavla Jendelová, Daniel Horák and Michal Babič are co-originators of a Eurasian patent no 015718 "Methods of preparation of superparamagnetic nanoparticles based on iron oxides with modified surface and superparamagnetic nanoparticles obtained by such a method" (2011). Pavla Jendelová, Karolina Turnovcová and Pavel Veverka are co-originators of the Czech patent application PV 2015-606 "Nanoparticles for magnetic and fluorescent labeling, their preparation, production and use".

Disclosure

The authors report no conflicts of interest in this work.

References

1. Nishikawa S, Goldstein RA, Nierras CR. The promise of human induced pluripotent stem cells for research and therapy. *Nat Rev Mol Cell Biol*. 2008;9(9):725–729.
2. de Lau LM, Breteler MM. Epidemiology of Parkinson's disease. *Lancet Neurol*. 2006;5(6):525–535.
3. Hawkes CH, Del Tredici K, Braak H. A timeline for Parkinson's disease. *Parkinsonism Relat Disord*. 2010;16(2):79–84.
4. Yan Y, Yang D, Zarnowska ED, et al. Directed differentiation of dopaminergic neuronal subtypes from human embryonic stem cells. *Stem Cells*. 2005;23(6):781–790.
5. Doi D, Samata B, Katsukawa M, et al. Isolation of human induced pluripotent stem cell-derived dopaminergic progenitors by cell sorting for successful transplantation. *Stem Cell Reports*. 2014;2(3):337–350.
6. Wernig M, Zhao JP, Pruszak J, et al. Neurons derived from reprogrammed fibroblasts functionally integrate into the fetal brain and improve symptoms of rats with Parkinson's disease. *Proc Natl Acad Sci U S A*. 2008;105(15):5856–5861.
7. Swistowski A, Peng J, Liu Q, et al. Efficient generation of functional dopaminergic neurons from human induced pluripotent stem cells under defined conditions. *Stem Cells*. 2010;28(10):1893–1904.
8. Grealish S, Diguet E, Kirkeby A, et al. Human ESC-derived dopamine neurons show similar preclinical efficacy and potency to fetal neurons when grafted in a rat model of Parkinson's disease. *Cell Stem Cell*. 2014;15(5):653–665.
9. Chambers SM, Fasano CA, Papapetrou EP, Tomishima M, Sadelain M, Studer L. Highly efficient neural conversion of human ES and iPS cells by dual inhibition of SMAD signaling. *Nat Biotechnol*. 2009;27(3):275–280.
10. Petit GH, Olsson TT, Brundin P. The future of cell therapies and brain repair: Parkinson's disease leads the way. *Neuropathol Appl Neurobiol*. 2014;40(1):60–70.
11. Payne NL, Sylvain A, O'Brien C, Herszfeld D, Sun G, Bernard CC. Application of human induced pluripotent stem cells for modeling and treating neurodegenerative diseases. *N Biotechnol*. 2015;32(1):212–228.
12. Miyoshi S, Flexman JA, Cross DJ, et al. Transfection of neuroprogenitor cells with iron nanoparticles for magnetic resonance imaging tracking: cell viability, differentiation, and intracellular localization. *Mol Imaging Biol*. 2005;7(4):286–295.
13. Chen CC, Ku MC, Jayaseema DM, Lai JS, Hueng DY, Chang C. Simple SPION incubation as an efficient intracellular labeling method for tracking neural progenitor cells using MRI. *PLoS One*. 2013;8(2):e56125.
14. Cromer Berman SM, Walczak P, Bulte JW. Tracking stem cells using magnetic nanoparticles. *Wiley Interdiscip Rev Nanomed Nanobiotechnol*. 2011;3(4):343–355.

15. Oh N, Park JH. Endocytosis and exocytosis of nanoparticles in mammalian cells. *Int J Nanomedicine*. 2014;9(suppl 1):51–63.
16. Kroll A, Pillukat MH, Hahn D, Schnekenburger J. Current *in vitro* methods in nanoparticle risk assessment: limitations and challenges. *Eur J Pharm Biopharm*. 2009;72(2):370–377.
17. Veverka M, Jirak Z, Kaman O, et al. Distribution of cations in nanosize and bulk Co-Zn ferrites. *Nanotechnology*. 2011;22(34):345701.
18. Babič M, Horak D, Trchova M, et al. Poly(L-lysine)-modified iron oxide nanoparticles for stem cell labeling. *Bioconjug Chem*. 2008;19(3):740–750.
19. Yu J, Vodyanik MA, Smuga-Otto K, et al. Induced pluripotent stem cell lines derived from human somatic cells. *Science*. 2007;318(5858):1917–1920.
20. Polentes J, Jendelová P, Cailleret M, et al. Human induced pluripotent stem cells improve stroke outcome and reduce secondary degeneration in the recipient brain. *Cell Transplant*. 2012;21(12):2587–2602.
21. Cho MS, Hwang DY, Kim DW. Efficient derivation of functional dopaminergic neurons from human embryonic stem cells on a large scale. *Nat Protoc*. 2008;3(12):1888–1894.
22. Novotna B, Turnovcova K, Veverka P, et al. The impact of silica encapsulated cobalt zinc ferrite nanoparticles on DNA, lipids and proteins of rat bone marrow mesenchymal stem cells. *Nanotoxicology*. 2016;10(6):662–670.
23. Horák D, Babič M, Jendelová P, et al. Effect of different magnetic nanoparticle coatings on the efficiency of stem cell labeling. *J Magn Magn Mater*. 2009;321(10):1539–1547.
24. Novotna B, Jendelová P, Kapcalova M, et al. Oxidative damage to biological macromolecules in human bone marrow mesenchymal stromal cells labeled with various types of iron oxide nanoparticles. *Toxicol Lett*. 2012;210(1):53–63.
25. Sanpo N, Berndt CC, Wen C, Wang J. Transition metal-substituted cobalt ferrite nanoparticles for biomedical applications. *Acta Biomater*. 2012;9(3):5830–5837.
26. Shabazi-Gahrouei D. *In vitro* evaluation of cobalt-zinc ferrite nanoparticles coated with DMSA on human prostate cancer cells. *J Mol Biomark Diagn*. 2013;4(3):154.
27. Ghasemian Z, Shahbazi-Gahrouei D, Manouchehri S. Cobalt zinc ferrite nanoparticles as a potential magnetic resonance imaging agent: an *in vitro* study. *Avicenna J Med Biotechnol*. 2015;7(2):64–68.
28. Guzman R, Uchida N, Bliss TM, et al. Long-term monitoring of transplanted human neural stem cells in developmental and pathological contexts with MRI. *Proc Natl Acad Sci U S A*. 2007;104(24):10211–10216.
29. Neri M, Maderna C, Cavazzin C, et al. Efficient *in vitro* labeling of human neural precursor cells with superparamagnetic iron oxide particles: relevance for in vivo cell tracking. *Stem Cells*. 2008;26(2):505–516.
30. Thu MS, Najbauer J, Kendall SE, et al. Iron labeling and pre-clinical MRI visualization of therapeutic human neural stem cells in a murine glioma model. *PLoS One*. 2009;4(9):e7218.
31. Ramos-Gomez M, Seiz EG, Martinez-Serrano A. Optimization of the magnetic labeling of human neural stem cells and MRI visualization in the hemiparkinsonian rat brain. *J Nanobiotechnology*. 2015;13:20.
32. Gutova M, Frank JA, D'Apuzzo M, et al. Magnetic resonance imaging tracking of ferumoxytol-labeled human neural stem cells: studies leading to clinical use. *Stem Cells Transl Med*. 2013;2(10):766–775.
33. Heyn C, Bowen CV, Rutt BK, Foster PJ. Detection threshold of single SPIO-labeled cells with FIESTA. *Magn Reson Med*. 2005;53(2):312–320.
34. Sharifi S, Seyednejad H, Laurent S, Atyabi F, Saei AA, Mahmoudi M. Superparamagnetic iron oxide nanoparticles for *in vivo* molecular and cellular imaging. *Contrast Media Mol Imaging*. 2015;10(5):329–355.
35. Park KI, Ourednik J, Ourednik V, et al. Global gene and cell replacement strategies via stem cells. *Gene Ther*. 2002;9(10):613–624.
36. Pluchino S, Quattrini A, Brambilla E, et al. Injection of adult neurospheres induces recovery in a chronic model of multiple sclerosis. *Nature*. 2003;422(6933):688–694.
37. Focke A, Schwarz S, Foerschler A, et al. Labeling of human neural precursor cells using ferromagnetic nanoparticles. *Magn Reson Med*. 2008;60(6):1321–1328.
38. Popescu IR, Nicaise C, Liu S, et al. Neural progenitors derived from human induced pluripotent stem cells survive and differentiate upon transplantation into a rat model of amyotrophic lateral sclerosis. *Stem Cells Transl Med*. 2012;2(3):167–174.
39. Kondo T, Asai M, Tsukita K, et al. Modeling Alzheimer's disease with iPSCs reveals stress phenotypes associated with intracellular Aβ and differential drug responsiveness. *Cell Stem Cell*. 2013;12(4):487–496.
40. Wang S, Bates J, Li X, et al. Human iPSC-derived oligodendrocyte progenitor cells can myelinate and rescue a mouse model of congenital hypomyelination. *Cell Stem Cell*. 2012;12(2):252–264.
41. Kola L, Landis J. Can the pharmaceutical industry reduce attrition rates? *Nat Rev Drug Discov*. 2004;3(8):5.
42. Compagnucci C, Nizzardo M, Corti S, Zanni G, Bertini E. *In vitro* neurogenesis: development and functional implications of iPSC technology. *Cell Mol Life Sci*. 2014;71(9):1623–1639.
43. Romanyuk N, Amemori T, Turnovcova K, et al. Beneficial effect of human induced pluripotent stem cell-derived neural precursors in spinal cord injury repair. *Cell Transplant*. 2015;24(9):1781–1797.
44. Hartfield EM, Yamasaki-Mann M, Ribeiro Fernandes HJ, et al. Physiological characterization of human iPS-derived dopaminergic neurons. *PLoS One*. 2014;9(2):e87388.
45. Eamegdool SS, Weible MW 2nd, Pham BT, Hawkett BS, Grieve SM, Chan-ling T. Ultrasmall superparamagnetic iron oxide nanoparticle prelabelling of human neural precursor cells. *Biomaterials*. 2014;35(21):5549–5564.
46. Tang H, Sha H, Sun H, et al. Tracking induced pluripotent stem cells-derived neural stem cells in the central nervous system of rats and monkeys. *Cell Reprogram*. 2012;15(5):435–442.
47. Abeliovich A, Hammond R. Midbrain dopamine neuron differentiation: factors and fates. *Dev Biol*. 2007;304(2):447–454.
48. Ferri AL, Lin W, Mavromatakis YE, et al. Foxa1 and Foxa2 regulate multiple phases of midbrain dopaminergic neuron development in a dosage-dependent manner. *Development*. 2007;134(15):2761–2769.
49. Cho MS, Lee YE, Kim JY, et al. Highly efficient and large-scale generation of functional dopamine neurons from human embryonic stem cells. *Proc Natl Acad Sci U S A*. 2008;105(9):3392–3397.
50. Noisa P, Raivio T, Cui W. Neural progenitor cells derived from human embryonic stem cells as an origin of dopaminergic neurons. *Stem Cells Int*. 2015;2015:10.